JCTC Journal of Chemical Theory and Computation

Assessment of Approximate Density Functional Methods for the Study of the Interactions of Al(III) with Aromatic Amino Acids

E. Rezabal,*,† T. Marino,‡ J. M. Mercero,† N. Russo,‡ and J. M. Ugalde†

Kimika Fakultatea, Euskal Herriko Unibertsitatea and Donostia International Physics Center (DIPC), P. K. 1072, 20080 Donostia, Euskadi, Spain, and Dipartimento di Chimica and Centro di Calcolo ad Alte Prestazioni per Elaborazioni Parallele e Distribuite - Centro d'Eccellenza MIUR, Universitá della Calabria, I-87030 Arcavacata di Rende (CS), Italy

Received February 2, 2007

Abstract: Four approximate Density Functional Theory methods, the standard hybrid B3LYP functional, the hybrid mPW1PW91 functional designed to account for van der Waals forces, the one-parameter meta hybrid TPSSh functional, the general-purpose meta hybrid MPWB1K functional and one Molecular Orbital Theory method, the standard Moller−Plesset perturbation theory up to second-order MP2, have been assessed for studying the complexation modes of the highly acidic Al(III) cation with the three aromatic amino acids, phenylalanine (Phe), tyrosine (Tyr), and tryptophan (Trp). Based on their performance toward the prediction of the geometrical structure of a number of lowest energy isomers and their relative binding energies, it is concluded that the B3LYP approximate functional renders the desired accuracy at the minimum computational cost.

1. Introduction

We concur with others[1] that Density Functional Theory (DFT) implementations are the most promising ab initio quantum mechanical methods for the computational study of large compounds, in general, and biologically relevant structures in particular.[2] However, it should be pointed out that DFT methods constitute a family of methods rather than a single method. Although Perdew's *Jacob's ladder* approach enables rationalizing the quality of the various DFT methods, a precise prescription to assess the quality of a given DFT method is still lacking. This is why given a particular system, selecting the most appropriate DFT method is so difficult and why validation and assessment of the various approximate DFT methods remain crucial for the reliability of the obtained data.

For biological systems, validation of the theoretical methods can be made by comparison of the calculated data against experimental data for a collection of *molecules containing atoms* commonly found in biomolecules.[2−4] Alternatively, one could also carry out the validation by selecting a number of relevant biomolecules themselves and then comparing the calculated DFT data against other accurate molecular structure methods.[5,6]

Our primary interest here is to substantiate the selection of a computationally cost-effective and accurate enough DFT method for the investigation of the aluminum metalloproteins. The relevance of aluminum in protein environments relies on the fact that aluminum, the most abundant metal on Earth—about 8% of the Earth's crust, is known to be toxic in biological environments. Thus, it is highly toxic to plant roots,[7] especially under acidic soil conditions, and it has also been related to several neurological disorders.[8] Since the bioavailability of aluminum has increased considerably, due to human intervention,[9,10] interest toward its biochemistry has increased recently.[11] However, despite this research effort, the molecular basis of the toxicity of aluminum are

* Corresponding author e-mail: pobrease@sc.ehu.es.
† Euskal Herriko Unibertsitatea and Donostia International Physics Center.
‡ Universitá della Calabria.

10.1021/ct700027n CCC: $37.00
Published on Web 07/03/2007

Table 1. Number of Isomers Characterized for the Aluminum Aromatic Amino Acids Complexes

	non cation-π				cation-π			
	bidentate					bidentate		
	N/O	N/OH	O/O	monodentate O	tridentate N/O/ring	N/ring	O/ring	total
Phe	2	1	1	1	1		2[a]	8
Tyr	2	1	1	1	1	1	2[a]	9
Trp	2				3[b]	2[c]	4[d]	11

[a] One isomer is charge solvated (cs) and the other is zwitterionic (zw). [b] Two isomers have covalent Al−ring bonding. [c] One isomer has covalent Al−ring bonding. [d] Two isomers are charge solvated (cs) and two isomers are zwitterionic (zw).

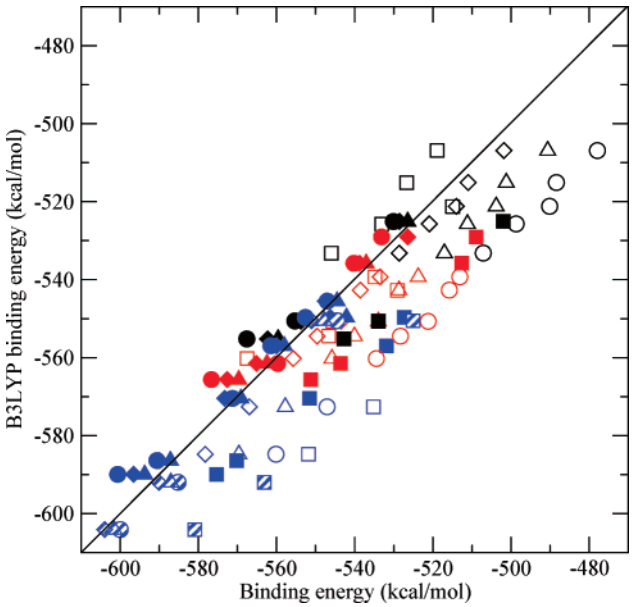

Figure 1. B3LYP binding enthalpies are presented on the *y*-axis, and binding enthalpies obtained by other methods on the *x*-axis, in kcal/mol. Black symbols regard Phe complexes, while red and blue symbols stand for Tyr and Trp ones, respectively. Squares represent MP2 results, triangles the mPW1PW91, circles the MPWB1K, and diamonds the TPSSh. Finally, empty figures symbolize the complexes without cation-π interaction and the filled ones the complexes with cation-π interaction. The striped blue symbols regard the Trp structures where the metal interacts covalently with the ring

still largely unknown. Consequently, a detailed investigation of the interactions of aluminum with amino acid residues constitutes an important piece of information that could help unveiling the behavior of the metal in protein environments.

The intricate three-dimensional structures that metalloproteins assume are largely determined by a delicate balance of a myriad of interactions between the residues and the protein's backbone with the metal.[12] Proteins containing aromatic amino acids rank high on the complexity scale of these interactions for they foster, in addition to ordinary covalent, ionic, and charge-transfer interactions, cation-π interactions between the metal and the aromatic part of their residues. Therefore, the aromatic amino acids (AAA) are well suited for assessing the reliability of a method for metalloprotein studies. Consequently, selection of a particular level of theory for reliable studies on these complex systems is more subtle than for the metal−amino acid complexes bearing less variety of interactions. Even more, experimental data concerning the binding energies of AAAs and cations, like Na^+, Li^+, and K^+,[13−16] and late transition metals,[17−30] Ag^+, Cu^+, and Zn^{2+}, can be found in the literature, suggesting that sensible data for aluminum could also be obtained similarly for the benefit of a reliable assessment. These amino acids, phenylalanine (Phe), tyrosine (Tyr), and tryptophan (Trp), account for 8.4% of the amino acids in proteins,[31] and the 26% of all Trp residues are known to be involved in energetically significant cation-π interactions.[32] Protein Data Bank (PDB) research has revealed the cation-π interaction to be widespread, also within the proteins.[32,33]

On the other hand, it is worth noticing that cation-π interactions in protein environments have been extensively studied for metals other than aluminum.[34] Thus, the open chemical literature contains numerous studies that underline their importance for the stabilization of the protein's geometry.[35−37] Several studies have also been devoted to investigate the nature of the cation-π interactions. Current consensus suggests that they are dominated by electrostatic forces[32,38,39] and cation-induced polarization terms,[40] which correlate with the magnitude of the quadrupole moment of the aromatic ring and the molecular polarizability of the aromatic compounds, respectively.[41−43]

Aluminum is expected to interact predominantly with the most electronegative parts of the AAAs, namely, the aromatic ring of the side chain and the carboxylate oxygens and the N atom of the backbone, giving rise to several isomeric structures, some of which present cation-π interactions and some of which do not. Finding a method that predicts accurately the relative energies between all these isomers is crucial for the subsequent biochemical interpretation. Consequently, our goal for the present study is to assess the reliability of a number of computational implementations of DFT for predicting reliably the relative stabilities of aluminum metalloproteins.

2. Methods

Among the long list of approximate density functionals, we have selected four. In first place comes the venerable B3LYP hybrid DFT approximate functional[44] which consists of the B3 exchange functional,[45] the LYP correlation functional,[46] and a 20% of exact exhange. It has already been well-established that this density functional implementation gives excellent results for most chemical systems[47] including cation-π interactions.[30,37,48−50] Second, we will consider the mPW1PW91 functional of Adamo and Barone.[51] This

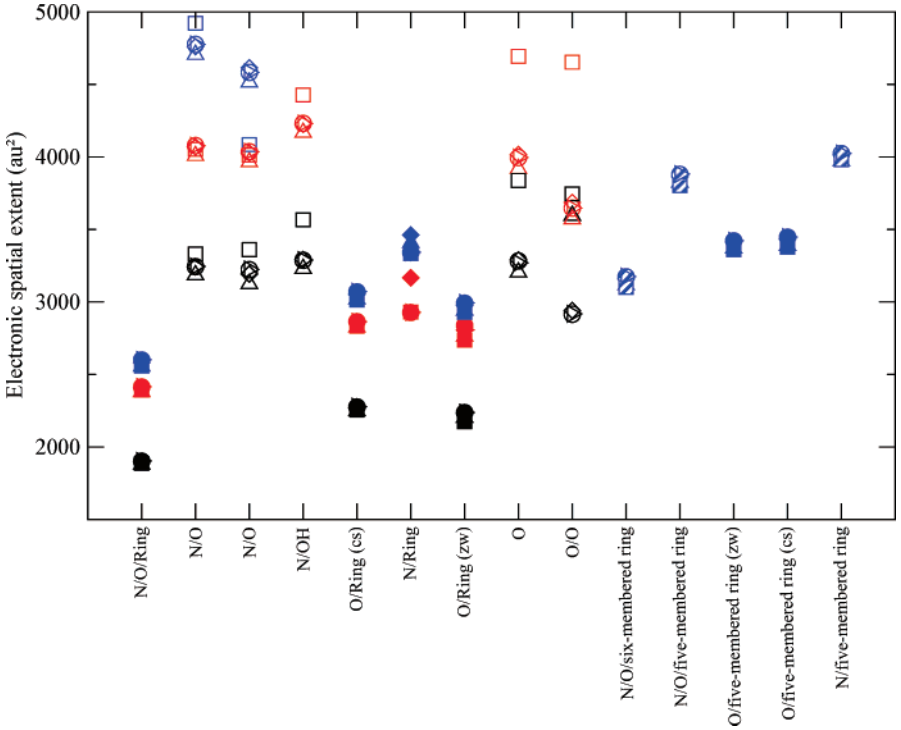

Figure 2. The electronic spatial extent as a function of the aluminum coordination mode for the three aromatic amino acids, black (Phe), red (Tyr), and blue (Trp). Empty and filled symbols represent complexes without and with intramolecular cation-π interaction, respectively. Squares stand for MP2, up triangles for mPW1PW91, circles for MPWB1K, diamonds for TPSSh, and right triangles for B3LYP levels of theory. The striped symbols stand for the Trp−aluminum complexes having a covalent bond between the metal on one aromatic carbon atom.

functional, which was specifically designed to account for van der Waals interactions, has been found to give excellent results, as confronted with experimental data, for molecules with intramolecular cation-π interactions.[29,52,53] Third, we have selected the promising hybrid meta approximate functional of Tao, Perdew, Staroverov, and Scuseria[54] which has been reported to provide highly accurate descriptions of a number of diverse systems and their properties.[55] Fourth, we have chosen to consider the MPWB1K hybrid *meta* approximate functional of Zhao and Thruhlar,[56−58] as a representative of the new-generation general-purpose functionals for applications in thermochemistry, kinetics, and noncovalent interactions.[3]

Additionally, we have also carried out full quantum mechanical analysis of the interactions between aluminum and the aromatic amino acids at the MP2 level of theory for it has been reported that it yields very satisfactory agreement with available spectroscopic experimental data of many biological molecules.[59]

All the calculations carried out in this research were performed with the Gaussian 03 code.[60] The structures were fully optimized at the B3LYP, mPW1PW91, TPSSh, and MP2 levels of theory, using the standard all-electron 6-31+G(d,p) basis for the aluminum ion, and the compact effective core potentials and shared-exponent basis set of Stevens, Basch, Krauss, and Jasien (SBKJ)[61] for C, N, O, and H. Gresh et al.[62−64] found that this pseudopotentials/all-electron basis set combination for the ligand and the metal cation, respectively, represents a very well balanced compromise between accuracy and computational efficiency. This method has been widely used in our group and has shown to be adequate for this type of calculations.[65−70] This basis set will hereafter be referred to as SBKJ/*+. Subsequent vibrational frequency analysis confirmed that structures were stable minima on their corresponding potential energy surface.

Single point calculations, at the optimized geometries, were carried out, with the considerably larger 6-311++G(2df,-2p) basis set, in order to improve the binding energies of the species considered, for the B3LYP, mPW1PW91, TPSSh, and MP2 levels of theory. For the MPWB1K approximate functional persistent geometry convergence problems were encountered. Consequently, at this level of theory single point calculation with the 6-311++G(2df,2p) basis set were carried out at the optimized B3LYP geometries. Nevertheless, it is worth mentioning that for all cases in which geometry convergence was achieved with the MPWB1K functional, the resulting structures were found to be remarkably similar to their corresponding optimized B3LYP ones. In the present work, the binding energy between an aromatic amino acid (AAA) and the aluminum cation is defined as the enthalpy change (ΔH) of the following process:

$$Al^{3+} + AAA \rightarrow (Al - AAA)^{3+} \qquad (1)$$

The measurement of the performance of the various levels of theory for the structural characterization task will be carried out by the analysis of the electronic spatial extent of the optimized geometry of all the properly characterized structures. The electronic spatial extent is defined as the

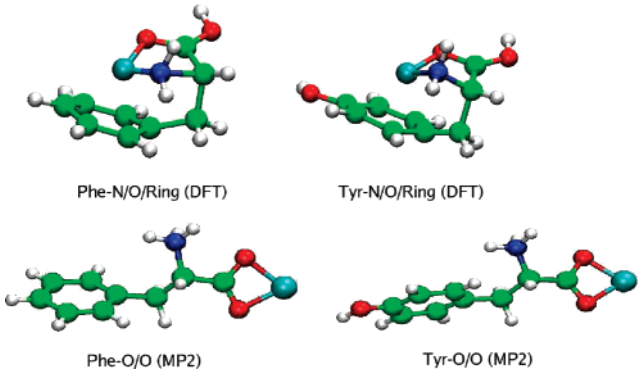

Figure 3. The most stable isomer of the Phe−Al^{+3} and Tyr−Al^{+3} complexes at the three B3LYP, mPW1PW91, MPWB1K, and TPSSh DFT levels of theory, top panel, and the most stable isomer of the Phe−Al^{+3} and Tyr−Al^{+3} complexes at the MP2 level of theory, bottom panel.

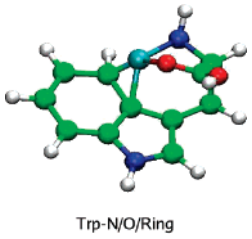

Figure 4. The most stable isomer of the Trp−Al^{+3} complex

expectation value, $\langle r^2 \rangle$, of the square modulus of the electronic vector **r** by the following equation

$$\langle r^2 \rangle = \int r^2 \rho(\mathbf{r}) d\mathbf{r} \qquad (2)$$

where $\rho(\mathbf{r})$ is the ground state electron density of the optimized structure.

3. Results and Discussion

We have fully characterized 28 stable minima structures for the aluminum aromatic amino acid complexes. Table 1 shows the rich structural variety of these isomers. In particular, 12 of them bear an intramolecular cation-π interaction. Remarkably, no stable structure was found neither for the N/OH or O/O bidentate nor for the O monodentate bonding modes of aluminum with tryptophan. Aluminum interacting with Trp is very prone to form bidentate complexes, where one of the interactions corresponds to a cation-π interaction, and the other one to the charge-transfer interaction with the carboxylic oxygen atom. Notice that of the four isomers found with this bonding mode, two are charged solvated, while the remaining two are charge separated zwitterionic like complexes. Additionally, Trp has another remarkable feature when interacting with aluminum. Namely, when the aminic nitrogen and the aromatic ring lie in the coordination sphere of aluminum, the metal can bind covalently one of the carbon atoms of the aromatic ring. Both the tridentate N/O/ring and the bidentate N/ring bonding modes of Trp show this feature.

Phenylalanine and tyrosine behave quite similarly in the metalation process by aluminum ion, as observed from Table 1. The only salient difference is that Phe does not form an N/ring bidentate cation-π complex with aluminum. Tryptophan behaves distinctively with respect to the remaining AAAs toward aluminum complexation.

The binding energies, as defined in eq 1, obtained with all five methods assessed for all the 28 structures have been arranged in Figure 1. We have chosen to represent the B3LYP binding energies on the *y*-axis and the mPW1PW91, MPWB1K, TPSSh, and MP2 binding energies on the *x*-axis.

Regarding the binding energies of the structures without cation-π intramolecular interaction (empty symbols in Figure 1) one can conclude that all four selected DFT approximate functionals behave similarly. It is worth noting that the empty triangles (mPW1PW91 binding energies), empty circles (MPWB1K binding energies), and emptly diamonds (TPSSh binding energies) lie parallel to the diagonal. Namely, mPW1PW91, MPWB1K, and TPSSh predict binding energies similar to B3LYP, and their relative binding energies are also predicted to be similar, for all 12 aluminum complexes with the three aromatic amino acids with no intramolecular cation-π interactions. Comparison with MP2 is also very satisfactory for all the structures except for the two N/O bidentate complexes of Trp. Observe that the blue empty squares of Figure 1 lie far off the diagonal.

The electronic spatial extents as measured by the expectation value, $\langle r^2 \rangle$, of the square modulus of the electronic vector **r** of the 28 structures characterized at the five levels of theory assessed are shown in Figure 2. Inspection of the figure reveals three salient points. First, the MP2 optimum geometry of the least stable N/O bidentate Trp−aluminum complex differs substantially from the three, B3LYP, mPW1PW91, and TPSSh, optimum DFT geometries. Observe Figure 2, where the right side blue empty square lies below the blue triangle, circle, and diamond. Second, the MP2 optimum geometries of both the O/O bidentate and the monodentate Phe−aluminum complexes are also different with respect to their corresponding B3LYP, mPW1PW91, and TPSSh optimum DFT geometries. Third, similarly, the MP2 optimum geometries of both the O/O bidentate and the monodentate Tyr−aluminum complexes differ with respect to their DFT counterparts.

Inspection of Figure 2 reveals one-fourth salient point. Namely, that the optimum geometries of the complexes bearing an intramolecular cation-π interaction are very similar for all five methods assessed. In particular we would like to point out the remarkable similarity among the optimum DFT structures. This is reflected also in the calculated binding energies. Observe how close to the diagonal (B3LYP binding energies) lie in Figure 1 the filled triangles (mPW1PW91 binding energies), the circles (MPWB1K binding energies), and the diamonds (TPPSh binding energies). Nevertheless, it is worth noticing that the N/ring bidentate Tyr−aluminum complex was not found within the mPW1PW91 level of theory.

The optimized MP2 geometries agree well with the B3LYP ones for the aluminum aromatic amino acid complexes characterized by the presence of cation-π interaction. Although the B3LYP overbinds all complexes by some 20

Table 2. Mean Absolute Deviations from the B3LYP Results of the Binding Energies $\epsilon^{\Delta H}$, in kcal/mol, and of the Electronic Spatial Extension $\epsilon^{\langle r^2 \rangle}$, in au^2 [a]

	mPW1PW91		MPWB1K		MP2		TPSSh	
	$\epsilon^{\Delta H}$	$\epsilon^{\langle r^2 \rangle}$	$\epsilon^{\Delta H}$	$\epsilon^{\langle r^2 \rangle}$	$\epsilon^{\Delta H}$	$\epsilon^{\langle r^2 \rangle}$	$\epsilon^{\Delta H}$	$\epsilon^{\langle r^2 \rangle}$
cation-π	2.52	46.87	5.31	3.65	20.58	45.96	4.06	33.83
no cation-π	15.29	121.19	28.35	2.11	12.86	346.75	4.48	16.92
overall	7.88	78.72	15.18	2.99	17.27	174.87	4.33	25.19

[a] The aluminum−AAA complexes bearing an intramolecular cation−π interaction and for those not bearing it. The overall mean absolute deviations are also given.

kcal/mol, the predicted relative stability of the various isomers is the same for both levels of theory.

Considering Trp complexes where the metal interacts covalently with a C atom of the indole side chain (blue stripped symbols), both mPW1PW91 and MPWB1K functionals predict a slightly smaller (∼3 kcal/mol and ∼7 kcal/mol, respectively) binding energy with respect to the B3LYP mark. The TPSSh binding energies, on the other hand, lie within ∼0.5 kcal/mol with respect to the corresponding B3LYP marks. The MP2 optimized geometries for these complexes are similar to the DFT ones. However, the MP2 binding energies are ∼30 kcal/mol smaller than the corresponding B3LYP values, although the predicted relative stability remains unaltered.

One final general observation is that isomers bearing a cation-π interaction are more stable than the ones that do not, irrespective of the DFT level of theory. The relative stability of the formers is slightly greater at mPW1PW91, MPWB1K, and TPSSh levels of theory, as compared with B3LYP. This difference is minimum in the later case. This feature has been reported by Dunbar[52] for monovalent Na^+, Mg^+, Al^+, and the first row transition-metal cations.

Regarding MP2 results, the preference for the cation-π bearing structures depends on the actual amino acid considered. For example, for both Phe− and Tyr−aluminum complexes, MP2 favors the bidentate O/O coordination mode for the aluminum shown in Figure 3. Conversely, all the three DFT approximate methods considered in the present study predict a tridentate N/O/ring structure for the lowest energy isomer. It is worth emphasizing that it is the latter coordination mode, the tridentate one, the one that has been observed in previous structural experimental characterizations[29,30,50] of complexes between aromatic amino acids and Li^+, Na^+, K^+, Cu^+, and Ag^+ cations. The better agreement with experiments carried out with related complexes sheds some confidence on the improved performance of the DFT methods over MP2 for these aluminum complexes. Additionally, we have carried out CCSD(T) single point calculations for these two Al(III)−Phe structures which have conformed the higher stability of the N/O/ring coordination mode with respect to the O/O coordination mode.

Instead, for aluminum−Trp complexes all four methods assessed concur that the lowest energy structure bears a cation-π interaction. The most stable conformation, for all the theory levels studied, is predicted to be the tridentate N/O/ring complex where the aluminum interacts covalently with one of the carbon atoms of the indole six-membered ring depicted in Figure 4

4. Conclusions

Table 2 shows the mean absolute deviations calculated for the two properties scrutinized in the present study for all the 28 isomers characterized as stable minima for the complexes involving aluminum and the aromatic amino acids. The reference data set has been chosen to consist of the B3LYP results. It is observed that for the relative binding energies the DFT methods scrutinized give similar and satisfactory deviations, in particular for the complexes bearing an intramolecular cation-π interaction. Additionally, TPSSh does very much like B3LYP also for the complexes not bearing cation-π interactions. The MP2 results deviate four times as much than TPSSh, five times as much than MPWB1K, and ten times as much than mPW1PW91 for the binding energy of the complexes bearing an intramolecular cation-π interaction.

The deviation for the electronic spatial extent is smaller for complexes bearing an intramolecular cation-π interaction than for those that do not. Although this deviation might appear large, it is worth noticing that, in the worst case, the electronic spatial extent for the structures without a cation-π interaction, $\epsilon^{\langle r^2 \rangle} = 346$ au^2, deviates less than 10% from the mean electronic spatial extent, ∼3500 au^2.

Therefore, we can conclude that for aluminum aromatic amino acid complexes no significant improvement is gained by using neither mPW1PW91, MPWB1K, or TPSSh nor MP2, as seen in the literature for other related systems.[30] Besides, geometry optimization and frequency calculations at the MP2 level of theory requires a considerable computational effort, and MPWB1K suffers from poor geometry convergence. Consequently, both B3LYP and TPSSh methods were concluded to be a good compromise between cost and accuracy for the study of aluminum−AAA complexes, involving isomers with and without cation-π interactions.

Acknowledgment. This research was funded by Euskal Herriko Unibertsitatea (the University of the Basque Country), Gipuzkoako Foru Aldundia (the Provincial Government of Guipuzkoa), and Eusko Jaurlaritza (the Basque Government). The SGI/IZO−SGIker UPV/EHU (supported by the National Program for the Promotion of Human Resources within the National Plan of Scientific Research, Development and Innovation − Fondo Social Europeo and MCyT) is greatfully acknowledged for assistance and generous allocation of computational resources. Financial support from the Universitá degli Studi della Calabria and Regione Calabria (POR Calabria 2000/2006, misura 3.16, progetto PROSICA) is also acknowledged. Authors wish to thank Dr. A. Rimola

(Universitat Autonoma de Barcelona) for his critical reading of the manuscript.

Supporting Information Available: Optimized geometries of all characterized stable isomers as well as their relative energies at the five levels of theory. This material is available free of charge via the Internet at http://pubs.acs.org.

References

(1) Perdew, J. P.; Ruzsinszky, A.; Tao, J.; Staroverov, V. N.; Scuseria, G. E.; Csonka, G. I. *J. Chem. Phys.* **2005**, *123*, 062201.

(2) Riley, K. E.; Holt, B. T. O.; Merz, K. M., Jr. *J. Chem. Theory Comput.* **2007**, *3*, 407.

(3) Zhao, Y.; Schultz, N. E.; Truhlar, D. G. *J. Chem. Theory Comput.* **2006**, *2*, 364.

(4) Antony, J.; Grimme, S. *Phys. Chem. Chem. Phys.* **2006**, *8*, 5287.

(5) Dudev, T.; Lim, C. *J. Phys. Chem. B* **2000**, *104*, 3692.

(6) Johnson, E. R.; Becke, A. D. *Chem. Phys. Lett.* **2006**, *432*, 600.

(7) Williams, R. *Coord. Chem. Rev.* **2002**, *228*, 93.

(8) Yokel, R. *Neurotoxicology* **2000**, *21*, 813.

(9) Exley, C.; Esiri, M. M. *J. Neurol. Neurosurg. Psychiatry* **2006**, *77*, 877.

(10) Exley, C.; Begum, A.; Woolley, M. P.; Bloor, R. N. *Am. J. Med.* **2006**, *119*, 276.

(11) Exley, C. *J. Inorg. Biochem.* **2005**, *99*, 1747.

(12) Ruan, C.; Yang, Z.; Hallowita, N.; Rodgers, M. T. *J. Phys. Chem. A* **2005**, *109*, 11539.

(13) Gapeev, A.; Dunbar, R. *J. Am. Chem. Soc*. **2001**, *123*, 8360.

(14) Gapeev, A.; Dunbar, R. *Int. J. Mass Spectrom.* **2003**, *227*, 825.

(15) Kish, M. M.; Ohanessian, G.; Wesdemiotis, C. *Int. J. Mass Spectrom.* **2003**, *227*, 509.

(16) Ruan, C.; Rodgers, M. *J. Am. Chem. Soc.* **2004**, *126*, 14600.

(17) Cerda, B.; Wesdemiotis, C. *J. Am. Chem. Soc.* **1995**, *117*, 9734.

(18) Hoyau, S.; Ohanessian, G. *J. Am. Chem. Soc.* **1997**, *119*, 2016.

(19) Gatlin, C. L.; Turecek, F.; Vaisar, T. *J. Mass Spectrom.* **1995**, *30*, 1605.

(20) Gatlin, C. L.; Turecek, F.; Vaisar, T. *J. Am. Chem. Soc.* **1995**, *117*, 3637.

(21) Wen, D.; Yalcin, R.; Harrison, A. G. *Rapid Commun. Mass Spectrom.* **1997**, *8*, 749.

(22) Lei, Q.; Amster, I. J. *J. Am. Soc. Mass Spectrom.* **1996**, *7*, 722.

(23) Yalcin, T.; Wang, J.; Wen, D.; Harrison, A. G. *J. Am. Soc. Mass Spectrom.* **1997**, *8*, 749.

(24) Lavanant, H.; Hoppilliard, Y. *J. Mass Spectrom*. **1997**, *32*, 1037.

(25) Lavanant, H.; Hecquet, E.; Hoppilliard, Y. *Int. J. Mass Spectrom.* **1999**, *185/186/187*, 11.

(26) Talaty, E. R.; Perera, B. A.; Gallardo, A. L.; Barr, J. M.; Stipdonk, M. J. V. *J. Phys. Chem. A* **2001**, *105*, 8059.

(27) Shoeib, T.; Cunje, A.; Hopkinson, A.; Siu, K. *J. Am. Soc. Mass Spectrom.* **2002**, *13*, 408.

(28) Shoeib, T.; Siu, K. M.; Hopkinson, A. C. *J. Phys. Chem. A* **2002**, *106*, 6121.

(29) Polfer, N. C.; Oomens, J.; Moore, D. T.; Helden, G.; Meijer, G.; Dunbar, R. *J. Am. Chem. Soc.* **2006**, *128*, 517.

(30) Polfer, N.; Oomens, J.; Dunbar, R. *Phys. Chem. Chem. Phys.* **2006**, *8*, 2744.

(31) Meadows, E.; De Wall, S.; Barbour, L. J.; Gokel, G. W. *J. Am. Chem. Soc.* **2001**, *123*, 3092.

(32) Gallivan, J.; Dougherty, D. *Proc. Natl. Acad. Sci. U.S.A.* **1999**, *96*, 9459.

(33) Minoux, H.; Chipot, C. *J. Am. Chem. Soc.* **1999**, *121*, 10366.

(34) De Wall, S. L.; Meadows, E. S.; Barbour, L. J.; Gokel, G. W. *Proc. Natl. Acad. Sci.* **2000**, *97*, 6271.

(35) Ma, J.; Dougherty, D. *Chem. Rev.* **1997**, *97*, 1303.

(36) Gokel, G. W.; DeWall, S. L.; Meadows, E. S. *Eur. J. Org. Chem.* **2000**, 2967.

(37) Rimola, A.; Rodríguez-Santiago, L.; Sodupe, M. *J. Phys. Chem. B* **2006**, *110*, 24189.

(38) Mecozzi, S.; West, A.; Dougherty, D. A. *Proc. Natl. Acad. Sci. U.S.A.* **1996**, *93*, 10566.

(39) Dougherty, D. A. *Science* **1996**, *271*, 163.

(40) Cubero, E.; Luque, F. J.; Orozco, M. *Proc. Natl. Acad. Sci. U.S.A.* **1998**, *95*, 5976.

(41) Garau, C.; Frontera, A.; Quinonero, D.; Ballester, P.; Costa, A.; Deya, P. M. *J. Phys. Chem. A* **2004**, *108*, 9423.

(42) Garau, C.; Frontera, A.; Quinonero, D.; Ballester, P.; Costa, A.; Deya, P. M. *Chem. Phys. Lett.* **2004**, *392*, 85.

(43) Garau, C.; Frontera, A.; Quinonero, D.; Ballester, P.; Costa, A.; Deya, P. M. *Chem. Phys. Lett.* **2004**, *399*, 220.

(44) Stephens, P. J.; Devlin, F. J.; Chabalowski, C. F.; Frisch, M. J. *J. Phys. Chem.* **1994**, *98*, 11623.

(45) Becke, A. D. *J. Chem. Phys.* **1993**, *98*, 5648.

(46) Lee, C.; Yang, W.; Parr, R. G. *Phys. Rev. B* **1988**, *37*, 785.

(47) Mercero, J. M.; Matxain, J. M.; Lopez, X.; York, D. M.; Largo, A.; Eriksson, L. A.; Ugalde, J. M. *Int. J. Mass Spectrom.* **2005**, *240*, 37.

(48) Reddy, A. S.; Sastry, G. N. *J. Phys. Chem. A* **2005**, *109*, 8893.

(49) Zhang, S.; Liu, L.; Fu, Y.; Guo, Q. *J. Mol. Struct.* **2005**, *757*, 37.

(50) Ryzhov, V.; Dunbar, R. C.; Cerda, B.; Wesdemiotis, C. *Am. Soc. Mass Spectrom.* **2000**, *11*, 1037.

(51) Adamo, C.; Barone, V. *J. Chem. Phys.* **1998**, *108*, 664.

(52) Dunbar, R. C. *J. Phys. Chem. A* **2002**, *106*, 7328.

(53) Oliveira, G.; Martin, J.; Proft, F.; Geerlings, P. *Phys. Rev. A* **1999**, *60*, 1034.

(54) Tao, J.; Perdew, J. P.; Staroverov, V. N.; Scuseria, G. E. *Phys. Rev. Lett.* **2003**, *91*, 146401.

(55) Staroverov, V. N.; Scuseria, G. E.; Tao, J.; Perdew, J. P. *J. Chem. Phys.* **2003**, *119*, 12129.

(56) Zhao, Y.; Tishchenko, O.; Truhlar, D. G. *J. Phys. Chem. B* **2005**, *109*, 19046.

(57) Zhao, Y.; Thrular, D. G. *J. Phys. Chem. A* **2004**, *108*, 6908.

(58) Zhao, Y.; Truhlar, D. G. *Phys. Chem. Chem. Phys.* **2005**, *7*, 2701.

(59) Gerber, R. B.; Chaban, G. M.; Gregurick, S. K.; Brauer, B. *Biopolymers* **2003**, *68*, 370.

(60) Frisch, M. J.; Trucks, G. W.; Schlegel, H. B.; Scuseria, G. E.; Robb, M. A.; Cheeseman, J. R.; Montgomery, J. A., Jr.; Vreven, T.; Kudin, K. N.; Burant, J. C.; Millam, J. M.; Iyengar, S. S.; Tomasi, J.; Barone, V.; Mennucci, B.; Cossi, M.; Scalmani, G.; Rega, N.; Petersson, G. A.; Nakatsuji, H.; Hada, M.; Ehara, M.; Toyota, K.; Fukuda, R.; Hasegawa, J.; Ishida, M.; Nakajima, T.; Honda, Y.; Kitao, O.; Nakai, H.; Klene, M.; Li, X.; Knox, J. E.; Hratchian, H. P.; Cross, J. B.; Bakken, V.; Adamo, C.; Jaramillo, J.; Gomperts, R.; Stratmann, R. E.; Yazyev, O.; Austin, A. J.; Cammi, R.; Pomelli, C.; Ochterski, J. W.; Ayala, P. Y.; Morokuma, K.; Voth, G. A.; Salvador, P.; Dannenberg, J. J.; Zakrzewski, V. G.; Dapprich, S.; Daniels, A. D.; Strain, M. C.; Farkas, O.; Malick, D. K.; Rabuck, A. D.; Raghavachari, K.; Foresman, J. B.; Ortiz, J. V.; Cui, Q.; Baboul, A. G.; Clifford, S.; Cioslowski, J.; Stefanov, B. B.; Liu, G.; Liashenko, A.; Piskorz, P.; Komaromi, I.; Martin, R. L.; Fox, D. J.; Keith, T.; Al-Laham, M. A.; Peng, C. Y.; Nanayakkara, A.; Challacombe, M.; Gill, P. M. W.; Johnson, B.; Chen, W.; Wong, M. W.; Gonzalez, C.; Pople, J. A. G*aussian 03, Revision C.02*; Gaussian, Inc.: Wallingford, CT, 2004.

(61) Stevens, W. J.; Krauss, M.; Basch, H.; Jasien, P. G. *Can. J. Chem.* **1992**, *70*, 612.

(62) Garmer, D. R.; Gresh, N. *J. Am. Chem. Soc.* **1994**, *116*, 3556.

(63) Gresh, N.; Stevens, W. J.; Krauss, M. *J. Comput. Chem.* **1995**, *16*, 843.

(64) Gresh, N.; Garmer, D. R. *J. Comput. Chem.* **1996**, *17*, 1481.

(65) San Sebastian, E.; Mercero, J. M.; Roland H. Stote, A. D.; Cossío, F. P.; Lopez, X. *J. Am. Chem. Soc.* **2005**.

(66) Mercero, J. M.; Fowler, J. E.; Ugalde, J. M. *J. Phys. Chem. A* **1998**, *102* (35), 7006.

(67) Mercero, J. M.; Matxain, J. M.; Rezabal, E.; Lopez, X.; Ugalde, J. M. *Int. J. Quantum Chem.* **2004**, *98*, 409.

(68) Mercero, J. M.; Fowler, J. E.; Ugalde, J. M. *J. Phys. Chem. A* **2000**, *104*, 7053.

(69) Rulised, L.; Vondrasek, J. *J. Inorg. Biochem.* **1998**, *71*, 115.

(70) Mercero, J. M.; Mujika, J. I.; Matxain, J. M.; Lopez, X.; Ugalde, J. M. *Chem. Phys.* **2003**, *295*, 175.

CT700027N